

The two dimensional classical anisotropic Heisenberg ferromagnetic model with nearest- and next-nearest neighbor interactions

M.E. Gouvêa^a and A.S.T. Pires

Departamento de Física, ICEX, Universidade Federal de Minas Gerais Belo Horizonte, CP 702, CEP 30123-970, MG, Brazil

Received 3 April 2001 and Received in final form 20 September 2001

Abstract. We use the self-consistent harmonic approximation (SCHA) to study the two-dimensional classical Heisenberg anisotropic (easy-plane) ferromagnetic model including nearest- and next-nearest neighbor exchange interactions. For temperatures much lower than the Kosterlitz-Thouless phase transition temperature T_{KT} , spin waves must be the most relevant excitations in the system and the SCHA must account for its behavior. However, for temperatures near T_{KT} , we should expect vortex pairs to be quite important. The effect of these vortex excitations on the phase transition temperature is included in our theory as a renormalization of the exchange interactions. Then, combining the SCHA theory to the renormalization effect due to vortex pairs, we calculate the dependence of T_{KT} as a function of the easy-plane anisotropies and exchange interactions.

PACS. 75.10.Hk Classical spin models – 75.40.Cx Static properties (order parameter, static susceptibility, heat capacities, critical exponents, etc.)

1 Introduction

Magnetic systems with reduced dimensionality have provided a basis for a great number of insights into the several roles thermal fluctuations play in driving phase transitions [1]. The XY model represents a particularly important example of such a system, impacting problems in disciplines ranging from particle field theory to materials science. For instance, recently, Stephens and Hu [2] have shown that the black hole phase transition is qualitatively similar to the Kosterlitz-Thouless (KT) transition in condensed matter. Condensed matter systems of atoms and molecules are usually easier to understand than their high energy counterparts such as strings or geons. Then, we can exploit the analogies between different systems to shine some light into the behavior of systems which are otherwise experimentally and theoretically intractable.

The KT theory has been applied to many physical systems, including magnetic compounds, superconducting and superfluid films, and, also, to two-dimensional (2D) arrays of coupled Josephson junctions [3]. Some of the notable properties of the XY model are the absence of long-range order, the presence of topological defects known as vortices, and the KT transition. The low temperature phase has only bound vortex-antivortex pairs and the phase transition is associated to the unbinding of these pairs [4]. Gupta and Baillie [3] have presented a qualitative confirmation of the role played by vortex-antivortex pairs in the KT scenario.

However, most of the theoretical work done on low dimensional magnetic systems has considered only nearest-neighbor (nn) interactions. The understanding thus obtained can change considerably when one considers interactions with longer range. For example, spin systems with long-range potentials decaying as r^{-p} have attracted theoretical attention during the last two decades due to the fact that those systems are related to the mesoscopic tunnel junctions problem [5]. It is now known that long-range attractive interactions can induce critical behavior in low dimensional systems – even in one-dimension (1D), where there is no phase transition if only nearest interactions are considered. Thus, for models describing systems with d dimensions and 2 spin components – as the planar rotator model – it has been theoretically proven [6] that for $d < p < 2d$, where d is the dimension of the system, an ordering phase transition exists at a finite temperature.

Our interest here is to study the anisotropic Heisenberg model in the square lattice with easy-plane anisotropy including the next-nearest neighbor (nnn) exchange interaction to our model (described in (7)). It has been argued [7] that real compounds approximating 2D behavior with planar anisotropy – of which Rb_2CrCl_4 is probably the best example – may be considered to be equivalent to ideal 2D XY systems [8]. In fact, a considerable amount of theoretical and numerical work has been directed to anisotropic Heisenberg systems and it is now very well accepted [9] that a Kosterlitz-Thouless-like transition is also observed in 2D systems with planar anisotropy. However, those investigations are usually restricted to models including only nearest exchange interactions. Real

^a e-mail: meg@aquila.fisica.ufmg.br

materials can require a model including interactions of longer range. For example, the investigation on the compound $\text{BaNi}_2(\text{PO}_4)_2$ has also revealed a 2D XY behavior but its magnetic properties deduced from magnetization, susceptibility, specific heat and neutron scattering experiments [10] are well understood by considering the following model Hamiltonian

$$H = - \sum_{i,j} J_{ij} \mathbf{S}_i \cdot \mathbf{S}_j + D \sum_i (S_i^z)^2 \quad (1)$$

with $D = 7.3$ K, $J_{ij} = J_1 = -2.2$ K for interactions between nearest neighbors, and $J_2 = 0.3$ K and $J_3 = -8.8$ K for second- and third-neighbors, respectively. Thus, it is important to extend the theoretical investigations to models including longer range interactions. Another motivation to study these models can be found in a recent work done by Kim and Carbotte [11] showing that the effective Hamiltonian for the phase fluctuations in an s-wave superconductors is an XY Hamiltonian including interactions up to third neighbors.

Here, we will investigate the effect due to the next-nearest neighbor interaction on the phase transition temperature and, also, on other properties like the spin-stiffness using an approximate method known as self-consistent harmonic approximation (SCHA). The effect of bound vortex pairs near the transition temperature will also be discussed.

The SCHA is a simple approximate method that gives reasonable agreement with more sophisticated theories and, also, with Monte Carlo data [12]. For this reason, it has been widely used in the literature despite the fact that it does not always provide the correct order of the transition; in fact, the SCHA always predicts a *first*-order transition. This feature is due to the fact that, in the procedure, correlation functions containing more than two operators are factorized into products of pair correlation functions that are determined self-consistently. Any such factorization process breaks down sufficiently close to the transition point where the correlations are large and, when using such approximations, we must be careful and check for consistency.

The method has been extensively discussed in the literature (see, for example, Ref. [13]) and it consists, basically, in replacing the Hamiltonian of the system by an effective harmonic Hamiltonian with temperature dependent renormalized parameters. For example, for the planar rotator model

$$H_{\text{PR}} = - \frac{JS^2}{2} \sum_{\mathbf{r}, \mathbf{a}} \cos(\phi_{\mathbf{r}+\mathbf{a}} - \phi_{\mathbf{r}}), \quad (2)$$

where $\phi_{\mathbf{r}}$ is the angle associated with each lattice site \mathbf{r} and \mathbf{a} denotes the nearest neighbors to each site, the Hamiltonian can be written in its continuum form as

$$H_{\text{PR}}^c = \frac{JS^2}{2} \int d^2r (\nabla\phi)^2 \quad (3)$$

where a constant term was absorbed into the definition of ground state energy. However, in writing (3), all anharmonic terms present in (2) were neglected. One way

to take into account these terms is to renormalize the exchange interaction constant J using instead $\rho_s J$, where ρ_s is the spin stiffness [14] which, for the planar rotator model is given by

$$\rho_s = \langle \cos(\phi_{\mathbf{r}} - \phi_{\mathbf{r}+\mathbf{a}}) \rangle. \quad (4)$$

The stiffness calculated using (4) in the SCHA formalism, jumps discontinuously to zero at a critical temperature T_c given by

$$T_c^{\text{SCHA}} = zJS^2/e \quad (5)$$

where z is the number of nearest neighbors in the lattice and e is the base of natural logarithms. The mean field approximation (MFA) applied to the planar rotator yields a second-order transition with a higher transition temperature

$$T_c^{\text{MF}} = zJS^2/2 \approx 1.36T_c^{\text{SCHA}}. \quad (6)$$

It is very well known that the MFA usually overestimates the transition temperature because thermal fluctuations due to long-wavelength spin waves are neglected. Obviously, being the SCHA an approximate method, we can expect that its estimates for the transition temperature of a specific model will also be above the exact value. Notice, however, that for the planar rotator model the value obtained *via* SCHA is lower than the one obtained *via* MFA. Nevertheless, for the 2D planar rotator in a square lattice ($z = 4$), both MFA and SCHA estimates for T_c are well above the Monte Carlo [15] prediction $T_c = 0.898JS^2$ and, also, the renormalization group calculation [16] $T_c = 0.917JS^2$. Here we have to remember that vortices play an important role in the transition occurring in the 2D planar rotator model and such excitations are not included in the MFA or in the standard SCHA formalism. As it will be discussed later in this paper, the effect of vortices can be added to the SCHA treatment and the obtained transition temperature for the 2D square lattice planar rotator model [17] is $T_c = 0.96JS^2$ which compares well to the Monte Carlo and renormalization values.

The SCHA has been very successful in describing several systems (see, for example, Refs. [18,19]), and, specially, many magnetic systems [20–23]. When applied to study the thermodynamics of the quantum 2D XY model, the method showed that quantum fluctuations work in the sense of reducing the KT transition temperature from the classical T_{KT} value. The SCHA estimate for the spin $S = 1/2$ case gave $T_{\text{KT}}/JS^2 = 0.30$ which compares well to the Monte Carlo prediction $T_{\text{KT}}/JS^2 = 0.35$ for the same model [24]. The method has also been applied to the planar rotator in two-dimensions with long-range interactions decaying as r^{-p} [23] and a good agreement to Monte Carlo results reported in the literature was found, as will be discussed later in this work.

In Section 2 we discuss the SCHA theory and the calculation of the spin stiffness. The screening effect due to vortex pairs and the critical temperature as a function of the model parameters are discussed in Section 3. Our conclusion is presented in Section 4.

2 The SCHA approximation

Our model is described by the following Hamiltonian

$$H = -\frac{J}{2} \sum_{\mathbf{r}} \left[\sum_{\mathbf{a}} (S_{\mathbf{r}}^x S_{\mathbf{r}+\mathbf{a}}^x + S_{\mathbf{r}}^y S_{\mathbf{r}+\mathbf{a}}^y + \lambda_1 S_{\mathbf{r}}^z S_{\mathbf{r}+\mathbf{a}}^z) + \sum_{\mathbf{b}} \alpha (S_{\mathbf{r}}^x S_{\mathbf{r}+\mathbf{b}}^x + S_{\mathbf{r}}^y S_{\mathbf{r}+\mathbf{b}}^y + \lambda_2 S_{\mathbf{r}}^z S_{\mathbf{r}+\mathbf{b}}^z) \right] \quad (7)$$

where the sum in \mathbf{r} runs over all sites of a square lattice, \mathbf{a} denotes the nearest-neighbors to each site \mathbf{r} and \mathbf{b} denotes the next-nearest neighbors. The easy-plane anisotropies are described by the λ_1 and λ_2 parameters and $J\alpha$ is the nnn exchange interaction.

There is an extensive literature describing the SCHA procedure [20], and, for this reason, we will only sketch the main steps leading to the expressions for the spin stiffness and other quantities. We start by writing the spin components in (7) in terms of the representation

$$\begin{aligned} S_{\mathbf{r}}^x &= S \sqrt{1 - \left(\frac{S_{\mathbf{r}}^z}{S}\right)^2} \cos \phi_{\mathbf{r}}, \\ S_{\mathbf{r}}^y &= S \sqrt{1 - \left(\frac{S_{\mathbf{r}}^z}{S}\right)^2} \sin \phi_{\mathbf{r}}, \end{aligned} \quad (8)$$

obtaining

$$\begin{aligned} H = -\frac{J}{2} \sum_{\mathbf{r}} \left\{ \sum_{\mathbf{a}} \left[S^2 \sqrt{1 - \left(\frac{S_{\mathbf{r}}^z}{S}\right)^2} \sqrt{1 - \left(\frac{S_{\mathbf{r}+\mathbf{a}}^z}{S}\right)^2} \right. \right. \\ \left. \left. \times \cos(\phi_{\mathbf{r}} - \phi_{\mathbf{r}+\mathbf{a}}) + \lambda_1 S_{\mathbf{r}}^z S_{\mathbf{r}+\mathbf{a}}^z \right] \right. \\ \left. + \alpha \sum_{\mathbf{b}} \left[S^2 \sqrt{1 - \left(\frac{S_{\mathbf{r}}^z}{S}\right)^2} \sqrt{1 - \left(\frac{S_{\mathbf{r}+\mathbf{b}}^z}{S}\right)^2} \right. \right. \\ \left. \left. \times \cos(\phi_{\mathbf{r}} - \phi_{\mathbf{r}+\mathbf{b}}) + \lambda_2 S_{\mathbf{r}}^z S_{\mathbf{r}+\mathbf{b}}^z \right] \right\}. \quad (9) \end{aligned}$$

Then, following the procedure explained in [21], we expand the above expression for the Hamiltonian in terms of $(S_{\mathbf{r}}^z)^2$ and $(\phi_{\mathbf{r}} - \phi_{\mathbf{r}'})^2$, and, after using the normal ordering procedure and collecting the quadratic terms, we obtain

$$\begin{aligned} H_0 = 2J \sum_{\mathbf{q}} \left\{ S^2 [\rho_a(1 - \gamma_{\mathbf{q}}^a) + \alpha \rho_b(1 - \gamma_{\mathbf{q}}^b)] \phi_{\mathbf{q}} \phi_{-\mathbf{q}} \right. \\ \left. + [(1 - \lambda_1 \gamma_{\mathbf{q}}^a) + \alpha(1 - \lambda_2 \gamma_{\mathbf{q}}^b)] S_{\mathbf{q}}^z S_{-\mathbf{q}}^z \right\} \quad (10) \end{aligned}$$

for the Fourier transform of the effective harmonic expression of the Hamiltonian. Notice that the renormalization by the stiffness affects only the terms on ϕ . In (10), the functions $\gamma_{\mathbf{q}}^a$ and $\gamma_{\mathbf{q}}^b$, and the spin stiffness ρ_a and ρ_b are

defined as follows

$$\gamma_{\mathbf{q}}^a = \frac{1}{2} (\cos q_x + \cos q_y); \quad (11)$$

$$\gamma_{\mathbf{q}}^b = \frac{1}{2} [\cos(q_x + q_y) + \cos(q_x - q_y)]; \quad (12)$$

$$\rho_a = \left[1 - \left\langle \left(\frac{S_{\mathbf{r}}^z}{S} \right)^2 \right\rangle \right] e^{-\frac{1}{2} \langle (\phi_{\mathbf{r}+\mathbf{a}} - \phi_{\mathbf{r}})^2 \rangle}; \quad (13)$$

$$\rho_b = \left[1 - \left\langle \left(\frac{S_{\mathbf{r}}^z}{S} \right)^2 \right\rangle \right] e^{-\frac{1}{2} \langle (\phi_{\mathbf{r}+\mathbf{b}} - \phi_{\mathbf{r}})^2 \rangle}. \quad (14)$$

In the calculation of ρ_a and ρ_b , we approximate $\langle \dots \rangle$ by $\langle \dots \rangle_0$, that is, we use the harmonic Hamiltonian H_0 to calculate the averages. This approximation results in treating $\phi_{\mathbf{r}}$ and $S_{\mathbf{r}}^z$ as uncoupled variables.

In order to obtain the total spin stiffness ρ and its relation to ρ_a and ρ_b , we write (9) in its continuum version

$$\begin{aligned} H^c = \frac{\tilde{J}}{2} \int d^2r \left\{ \frac{S^2(\rho_a + 2\alpha\rho_b)}{1 + 2\alpha} (\nabla\phi)^2 + (\nabla S^z)^2 \right. \\ \left. + \frac{[(1 - \lambda_1) + 2\alpha(1 - \lambda_2)] S^z \nabla^2 S^z}{1 + 2\alpha} \right\}, \quad (15) \end{aligned}$$

where $\tilde{J} = J(1 + 2\alpha)$. Then, we conclude that the total spin stiffness is given by the factor multiplying the term depending on ϕ , that is

$$\rho = \frac{\rho_a + 2\alpha\rho_b}{1 + 2\alpha}. \quad (16)$$

The averages appearing in (13) and (14) can be calculated if we introduce a Bogoliubov transformation

$$\begin{aligned} \phi_{\mathbf{q}} &= \frac{1}{\sqrt{2}} \left\{ \frac{(1 - \lambda_1 \gamma_{\mathbf{q}}^a) + \alpha(1 - \lambda_2 \gamma_{\mathbf{q}}^b)}{S^2[\rho_a(1 - \gamma_{\mathbf{q}}^a) + \alpha\rho_b(1 - \gamma_{\mathbf{q}}^b)]} \right\}^{1/4} [a_{\mathbf{q}}^\dagger + a_{-\mathbf{q}}] \\ S_{\mathbf{q}}^z &= i \frac{1}{\sqrt{2}} \left\{ \frac{S^2[\rho_a(1 - \gamma_{\mathbf{q}}^a) + \alpha\rho_b(1 - \gamma_{\mathbf{q}}^b)]}{(1 - \lambda_1 \gamma_{\mathbf{q}}^a) + \alpha(1 - \lambda_2 \gamma_{\mathbf{q}}^b)} \right\}^{1/4} [a_{\mathbf{q}}^\dagger - a_{-\mathbf{q}}], \end{aligned} \quad (17)$$

where a^\dagger and a are the creation and annihilation operators. This procedure is standard in spin wave theories and leads us to the renormalized spin wave dispersion relation

$$\begin{aligned} \omega_{\mathbf{q}} = 4JS \left\{ [\rho_a(1 - \gamma_{\mathbf{q}}^a) + \alpha\rho_b(1 - \gamma_{\mathbf{q}}^b)] \right. \\ \left. \times (1 - \lambda_1 \gamma_{\mathbf{q}}^a) + \alpha(1 - \lambda_2 \gamma_{\mathbf{q}}^b) \right\}^{1/2}, \quad (18) \end{aligned}$$

as well as to the expressions for the averages appearing in (13) and (14) giving

$$\begin{aligned} \rho_a = \left[1 - \frac{T}{4JS^2} I(\lambda_1, \lambda_2) \right] \\ \times \exp \left\{ -\frac{1}{(2\pi)^2} \frac{T}{4JS^2} \int d^2q \frac{(1 - \gamma_{\mathbf{q}}^a)}{\rho_a(1 - \gamma_{\mathbf{q}}^a) + \alpha\rho_b(1 - \gamma_{\mathbf{q}}^b)} \right\}, \quad (19) \end{aligned}$$

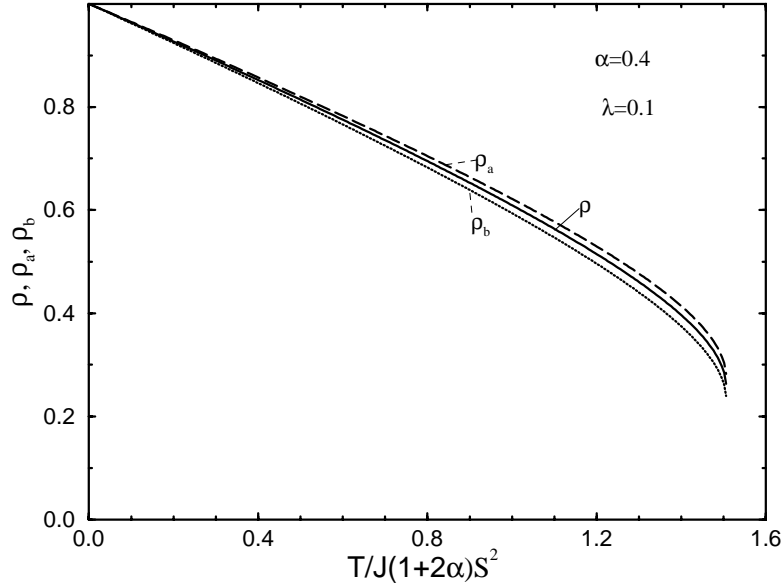


Fig. 1. Temperature dependence of the spin stiffness for $\alpha = 0.4$ and $\lambda_1 = \lambda_2 = 0.1$. The continuous line corresponds to ρ . The dashed and dotted lines correspond, respectively, to ρ_a and ρ_b as explained in the text.

$$\rho_b = \left[1 - \frac{T}{4JS^2} I(\lambda_1, \lambda_2) \right] \times \exp \left\{ -\frac{1}{(2\pi)^2} \frac{T}{4JS^2} \int d^2q \frac{(1 - \gamma_{\mathbf{q}}^b)}{\rho_a(1 - \gamma_{\mathbf{q}}^a) + \alpha\rho_b(1 - \gamma_{\mathbf{q}}^b)} \right\} \quad (20)$$

where

$$I(\lambda_1, \lambda_2) = \frac{1}{(2\pi)^2} \int d^2q \frac{1}{(1 - \lambda_1 \gamma_{\mathbf{q}}^a) + \alpha(1 - \lambda_2 \gamma_{\mathbf{q}}^b)}. \quad (21)$$

Equations (19–21) can then be solved self-consistently and allow us to determine the stiffness ρ , given by (16), for each temperature.

3 The renormalization by vortex pairs and the phase transition

In Figure 1, we show the dependence of ρ_a , ρ_b and the total spin stiffness ρ on the temperature T/J for $\alpha = 0.40$ and $\lambda_1 = \lambda_2 = 0.10$. After some temperature T_{\max} , the expressions for ρ_a and ρ_b , equations (19, 20), do not have any solution except the trivial one ($\rho_a = \rho_b = 0$). The abrupt disappearance of the stiffness ρ can be thought as signaling the break down of spin-wave like excitations and, thus, the disappearance of phase ordering. Using a long wavelength approximation for the integral in the argument of the exponential in equations (19, 20), we obtain, in the classical limit

$$\rho = \frac{[1 - \Theta I(\lambda_1, \lambda_2)]}{1 + 2\alpha} e^{-\frac{\Theta}{\rho_a + 2\alpha\rho_b}} \left(1 + 2\alpha e^{-\frac{\Theta}{\rho_a + 2\alpha\rho_b}} \right), \quad (22)$$

where $\Theta = T/(4JS^2)$. From this equation, we can determine that T_{\max} is given by

$$\frac{T_{\max}}{JS^2} = \frac{4}{\frac{e^x}{x(1+2\alpha e^{-x})} + I(\lambda_1, \lambda_2)}, \quad (23)$$

with x being determined by solving the equation $(1-x) + 2\alpha e^{-x}(1-2x) = 0$ for each α . Accepting T_{\max} as a first estimate of the transition temperature ($T_{\max} \rightarrow T_c$), we can easily conclude that for $\alpha = 0$, that is, the nearest neighbor model, we have $x = 1$ and the transition temperature is given by

$$T_c(\lambda) = \frac{4JS^2}{e + I(\lambda_1)}, \quad (24)$$

which is the same equation obtained in [21] (for $\alpha = 0$, $I(\lambda_1, \lambda_2) \rightarrow I(\lambda_1)$). We remind that, for the planar rotator model, $I(\lambda_1, \lambda_2) = 0$ and, from equations (23, 24), we can also conclude [21] that, due to the out-of-plane fluctuations, the transition temperature for the planar rotator model is higher than the one for the XY model; particularly, $T_c = 1.47JS^2$ for the nm ($\alpha = 0$) planar rotator while $T_c = 1.08JS^2$ for the classical XY model ($\alpha = \lambda_1 = 0$). For $\alpha \neq 0$ and $\lambda_1 = \lambda_2 = 0$, we have $I(\lambda_1, \lambda_2) = 1$ and, from (23) we obtain T_c as a function of α . This result is shown by the continuous line in Figure 2 where we see that the transition temperature increases almost linearly with α .

The dependence of T_c on the anisotropy parameters is contained in the function $I(\lambda_1, \lambda_2)$. For $\lambda_1 = \lambda_2 = \lambda \rightarrow 1$, we have

$$I(\lambda, \lambda) = \text{const.} + \frac{1}{\pi\lambda(1+2\alpha)} \ln(1-\lambda)^{-1} \quad (25)$$

meaning that as $\lambda \rightarrow 1$, the transition temperature goes to zero as $1/\ln[(1-\lambda)^{-1}]$. The same behavior was ob-

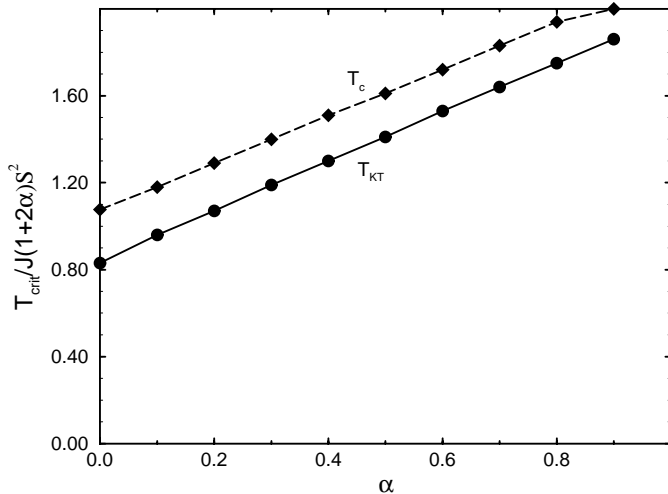


Fig. 2. Values obtained for T_c (SCHA theory — dashed line) and T_{KT} (SCHA + vortices — continuous line) as functions of the α parameter for $\lambda_1 = \lambda_2 = 0$.

tained by Nelson and Pelcovits [25] using the renormalization group technique. Their result does not depend on explicitly including nnn interactions or not and could be expected to hold for the model we are considering here. However, it is interesting that the simple SCHA is able to achieve to results obtained using a much more sophisticated theory.

The SCHA described in the previous section provides a way to include anharmonic corrections in the quadratic Hamiltonian (10) but, due to its nature, it is completely unable to incorporate the effect of bound vortex pairs — the essential ingredient in a KT-like transition. It is well known [26] that vortices only appear in a small range of temperatures in the vicinity of T_{KT} . Thus, for temperatures $T < \tilde{J}$, few vortex pairs exist and spin waves must be the main feature in the system; meaning that ρ must incorporate the relevant corrections to the dispersion relation. However, as $T \rightarrow T_c$, the number of vortex pairs increases exponentially and their effect on the dynamics becomes more important. The spin-wave and vortex contribution are apparently uncoupled and Kosterlitz and Thouless [27] have found that the vortices effects is to renormalize the spin-wave part. Later, Côté and Griffin [28] developed a theory analogous to the one used in classical electro-dynamics of continuous media and suggested that the vortex pairs effect can be thought as a dielectric function ϵ . Then, the effect of the bound pairs can be taken into account by a second renormalization of the exchange constant as schematically represented below

$$\tilde{J} \xrightarrow{\text{(SCHA)}} \tilde{J}\rho \xrightarrow{\text{vortices}} \frac{\tilde{J}\rho}{\epsilon} = J_T. \quad (26)$$

There is no explicit calculation of the dielectric function but it has been shown [16, 29] that ϵ^{-1} exhibits a universal

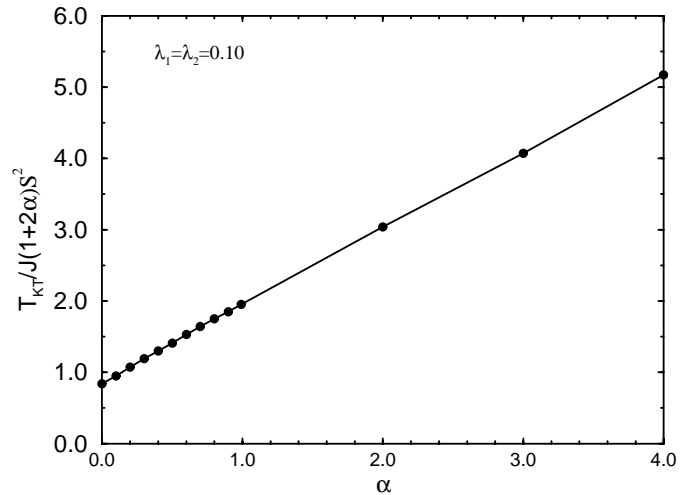


Fig. 3. T_{KT} as a function of α for $\lambda_1 = \lambda_2 = 0.1$

jump at $T = T_{KT}$, in the long wavelength limit, given by

$$\lim_{T \rightarrow T_{KT}^-} \frac{J_T(T)}{T} = \frac{2}{\pi}. \quad (27)$$

One way to incorporate the vortex contribution is to obtain the Kosterlitz-Thouless like temperature by the crossing between the $\rho(T)$ curve and the line $\gamma = J_T = 2T/[\pi(1+2\alpha)]$.

The dotted line in Figure 2 shows T_{KT} as a function of α for $\lambda_1 = \lambda_2 = 0$: we see that the inclusion of vortex pairs effects leads to a lower estimate for the transition temperature. For the nn planar rotator, the inclusion of the renormalization due to vortices [17] leads to $T_{KT} = 0.96JS^2$ which approaches better to the estimates $T_{KT} = 0.898JS^2$ obtained *via* Monte Carlo [15] and $T_{KT} = 0.917JS^2$ obtained by renormalization group techniques [16]. Similarly, for the nn XY model, we obtain $T_{KT} = 0.83JS^2$, in better agreement with the value $T_{KT} = 0.725JS^2$ obtained *via* Monte Carlo simulation [30] than the value obtained without including the vortex contribution. Figure 2 shows that the curves for T_c and T_{KT} as functions of α are almost parallel but the difference between T_c and T_{KT} decreases slightly as $\alpha \rightarrow 1$. Figure 3 also shows $T_{KT} \times \alpha$ but for $\lambda = 0.1$: there is no meaningful difference between the data shown in that figure for T_{KT} and the corresponding ones for $\lambda_1 = \lambda_2 = 0$ (Fig. 2). In Figure 4, we took $\alpha = 0.1$ and varied the anisotropy parameter: we observe, as discussed above, that the transition temperature varies very slowly with λ , except at the close vicinity of the isotropic limit $\lambda \rightarrow 1$. Analysing Figure 4 we understand why Figures 2 and 3 are so similar: the behavior of T_{KT} for $\alpha = 0$ and for $\alpha = 0.1$ cannot be expected to differ appreciably.

The increasing of the transition temperature as α , the strength of the nnn interaction, increases could be expected since, in the case being considered, the effect of the nnn interaction is basically to enhance the effective coupling constant. It is interesting to note that the results

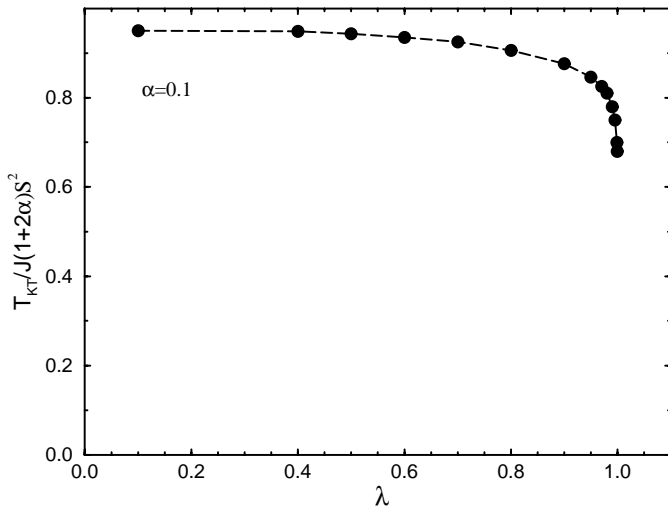


Fig. 4. T_{KT} as function of $\lambda_1 = \lambda_2 = \lambda$ for $\alpha = 0.1$.

displayed in Figures 2, 3 and 4 suggest that the inclusion of the nnn interaction results in a kind of scaling of the transition temperature with $(1 + 2\alpha)$ this result is similar to the one found in [11]. Obviously, the nature of the approximations inherent to the SCHA do not allow us to extract decisive conclusions about the existence of such scaling; further checking by other methods as, for example, Monte Carlo simulations, would be required.

4 Conclusion

In this paper, we used the SCHA to treat the anisotropic model with nn and nnn exchange interactions. We have already applied the SCHA to several systems with easy-plane anisotropy [20–23], and the comparison between SCHA results and results obtained by more precise techniques is very encouraging — despite the fact that the SCHA estimates for transition temperatures are almost always above the ones obtained by Monte Carlo or renormalization group approaches. In [20], we studied the 2D XY quantum and classical models combining the SCHA with the renormalization due to vortices as has also been done in this work (Sect. 3): the results describe the effect of quantum fluctuations in lowering T_c and compare quite well to existing Monte Carlo results. The effect of *interplanar* interaction in XY models was also studied [22] by the SCHA and the overall behavior obtained for the dependence of T_c as a function of the interplanar coupling resembles the one obtained by Monte Carlo simulations. Long-range interactions in the 2D planar rotator model were also studied in [23] with the SCHA. The model Hamiltonian used in [23] is given by

$$H = - \sum_{\mathbf{r}, \mathbf{r}'} J_{\mathbf{r}, \mathbf{r}'} (S_{\mathbf{r}}^x S_{\mathbf{r}'}^x + S_{\mathbf{r}}^y S_{\mathbf{r}'}^y) \quad (28)$$

where $J_{\mathbf{r}, \mathbf{r}'} = J|\mathbf{r} - \mathbf{r}'|^{-p}$, and, obviously, is quite different from the Hamiltonian considered in this work. Concerning (28), theoretical results [6] have proven that there

exists an ordering transition at a finite temperature for $2 < p < 4$, whereas for $p \geq 4$ the existing theorems [31] do not rule out the possibility of having a KT-like transition. In [23], we considered $p = 3, 4$ and 5 obtaining a quite good comparison to Romano's data [32] — who also found some evidence of KT-like transition for $p = 4$.

The present work gives continuity to our investigation of 2D easy plane models. Unfortunately, we could not check the results obtained with the approximations made here by comparing them to other results. However, the fact that the results behave like it could be expected for the model under investigation, added to the experience that has been accumulated in dealing with SCHA leads us to suggest that there is a KT-like transition whose temperature scales with $(1 + 2\alpha)$.

It is important to remark that the SCHA is a very simple method that, as shown in this work, can be easily extended to different models — as may be required to treat real magnetic materials where anisotropies, long range interactions, etc., may be important to correctly describe their behavior. For example, a proper analysis of the $\text{BaNi}_2(\text{PO}_4)_2$ compound should require the inclusion of interactions up to third neighbors — at least — since the ratio $\alpha' = J_3/J_1 = 4$ is much higher than $\alpha = 0.14$. Although it is not a difficult task to improve the model used in this work adding this interaction, we can expect that the major effect will be an increasing of the effective constant describing the exchange interaction. Following the steps discussed here, we can guess that the SCHA will give $J_1(1 + 2\alpha + 4\alpha')$ as the estimate for the effective exchange constant. Then, using $T_{KT} = 0.725JS^2$ for easy-plane models and adopting for J this estimate, we obtain $T_{KT} = 26.2$ K — which agrees quite well to the estimate done by Regnault *et al.* [8] ($T_{KT} \approx 23$ K).

Finally, it is also important to note that SCHA represents an improvement over the usual MFA because it does not neglect fluctuations due to long-wavelength spin waves. These features indicate that the use of SCHA can be very helpful to theoreticians and experimentalists interested in getting some insight about a model.

This work was partially supported by CNPq (Conselho Nacional para o Desenvolvimento da Pesquisa).

References

1. R.L. Leheny, R.J. Christianson, R.J. Birgeneau, R.W. Erwin, Phys. Rev. Lett. **82**, 418 (1999).
2. G.S. Stephens, B.L. Hu, *cond-mat/0102052*.
3. R. Gupta, C.F. Baillie, Phys. Rev. B **45**, 2883 (1992).
4. For a recent discussion about the KT transition see A.J. Chorin, Physica D **99**, 442 (1997).
5. R. Brown, E. Šimánek, Phys. Rev. B **34**, 2957 (1986); Phys. Rev. B **38**, 9264 (1988).

6. Ya.G. Sinai, *Theory of Phase Transitions: Rigorous Results* (Pergamon, Oxford, 1982).
7. S.T. Bramwell, P.C.W. Holdsworth, *J. Appl. Phys.* **73**, 6096 (1993).
8. L.P. Regnault, J. Rossat-Mignod in: *Magnetic Properties of Layered Transition Metal Compounds*, edited by L.J. de Jongh, R.D. Willet (Kluwer, Dordrecht, 1990), p. 271.
9. C. Kawabata, A.R. Bishop, *Sol. State Comm.* **42**, 595 (1982).
10. L.P. Regnault, J.P. Boucher, J. Rossat-Mignod, J. Bouillot, R. Pynn, J.Y. Henry, J.P. Renard, *Physica B* **136**, 329 (1986).
11. W. Kim, J.P. Carbotte, *cond-mat/0111122* (2001).
12. D.M. Wood, D. Stroud, *Phys. Rev. B* **25**, 1600 (1982).
13. J. Villain, *J. Phys. (France)* **35**, 27 (1974).
14. V.L. Pokrovsky, G.V. Uimin, *Zh. Eksp. Teor. Fiz.* **65**, 1691 (1973) [*Sov. Phys. JETP* **38**, 847 (1974)].
15. J. Tobochnik, G.V. Chester, *Phys. Rev. B* **20**, 3761 (1979).
16. T. Ohta, D. Jasnow, *Phys. Rev. B* **20**, 139 (1979).
17. Y.E. Lozovik, S.G. Akopov, *J. Phys. C* **14**, L31 (1981).
18. R.S. Fishman, *Phys. Rev. B* **38**, 11996 (1988).
19. E. Pytte, *Phys. Rev. Lett.* **28**, 895 (1972).
20. A.S.T. Pires, *Phys. Rev. B* **53**, 235 (1996).
21. A.S.T. Pires, M.E. Gouvêa, *Phys. Rev. B* **48**, 12698 (1993).
22. B.V. Costa, A.R. Pereira, A.S.T. Pires, *Phys. Rev. B* **54**, 3019 (1996).
23. M.E. Gouvêa, A.S.T. Pires, *J. Mag. Magn. Mat.* **162**, 225 (1996).
24. H.Q. Ding, *Phys. Rev. B* **45**, 230 (1992); M.S. Makivic, *Phys. Rev. B* **46**, 3167 (1992).
25. R.D. Nelson, R.A. Pelcovits, *Phys. Rev. B* **16**, 2192 (1977).
26. H. Weber, H.J. Jensen, *Phys. Rev. B* **44**, 454 (1991).
27. J.M. Kosterlitz, D.J. Thouless, *J. Phys. C* **6**, 1181 (1973).
28. R. Côté, A. Griffin, *Phys. Rev. B* **34**, 6240 (1986).
29. R.D. Nelson, J.M. Kosterlitz, *Phys. Rev. Lett.* **39**, 1201 (1977).
30. H.G. Evertz, D.P. Landau, in *Computer Simulation Studies in Condensed Matter Physics VIII*, edited by D.P. Landau, K.K. Mon, H.B. Schuettler [Springer, New York, 1995], p. 175.
31. J.B. Rogers, C.J. Thompson, *J. Stat. Phys.* **25**, 669 (1981).
32. S. Romano, *Phys. Rev. B* **42**, 8647 (1990); *Phys. Rev. B* **46**, 5420 (1992).